Optineurin promotes autophagosome formation by recruiting the autophagy-related Atg12-5-16L1 complex to phagophores containing the Wipi2 protein

Received for publication, June 13, 2017, and in revised form, October 31, 2017 Published, Papers in Press, November 13, 2017, DOI 10.1074/jbc.M117.801944

Megha Bansal[‡], Shivranjani C. Moharir[‡], S. Purnima Sailasree[‡], Kapil Sirohi[‡1], Cherukuri Sudhakar[‡], D. Partha Sarathi[‡], B. Jyothi Lakshmi[‡], Mario Buono[§], Satish Kumar[‡], and Ghanshyam Swarup[‡2]

From the [‡]Council of Scientific and Industrial Research (CSIR), Centre for Cellular and Molecular Biology, Hyderabad-500007, India and [§]MRC Molecular Hematology Unit, University of Oxford, Oxford OX3 9DS, United Kingdom

Edited by George N. DeMartino

Autophagy is a quality-control mechanism that helps to maintain cellular homeostasis by removing damaged proteins and organelles through lysosomal degradation. During autophagy, signaling events lead to the formation of a cup-shaped structure called the phagophore that matures into the autophagosome. Recruitment of the autophagy-associated Atg12-5-16L1 complex to Wipi2-positive phagophores is crucial for producing microtubule-associated protein 1 light chain 3-II (LC3-II), which is required for autophagosome formation. Here, we explored the role of the autophagy receptor optineurin (Optn) in autophagosome formation. Fibroblasts from Optn knock-out mouse showed reduced LC3-II formation and a lower number of autophagosomes and autolysosomes during both basal and starvation-induced autophagy. However, the number of Wipi2-positive phagophores was not decreased in Optn-deficient cells. We also found that the number of Atg12/16L1-positive puncta and recruitment of the Atg12-5-16L1 complex to Wipi2-positive puncta are reduced in Optn-deficient cells. Of note, Optn was recruited to Atg12-5-16L1–positive puncta, and interacted with Atg5 and also with Atg12-5 conjugate. A disease-associated Optn mutant, E478G, defective in ubiquitin binding, was also defective in autophagosome formation and recruitment to the Atg12-5-16L1–positive puncta. Moreover, we noted that Optn phosphorylation at Ser-177 was required for autophagosome formation but not for Optn recruitment to the phagophore. These results suggest that Optn potentiates LC3-II production and maturation of the phagophore into the autophagosome, by facilitating the recruitment of the Atg12-5-16L1 complex to Wipi2-positive phagophores.

Macroautophagy, called autophagy here, is an evolutionarily conserved cellular degradative process, which represents pathways leading to lysosomal degradation of cytoplasmic constituents, from macromolecules to organelles (1, 2). It is also involved in development, immunity, and clearance of invading microorganisms and its impairment contributes to several diseases (1, 3). Generally autophagy occurs at a basal level, and it is enhanced by several types of stresses, such as starvation, damaged organelles, abnormal proteins, and invading pathogens (4). Autophagy is initiated by signaling events that lead to formation of a cup-shaped double membrane structure known as phagophore (isolation membrane), which matures into autophagosome (1, 5). Many autophagy-related (Atg) proteins in yeast and mammals form the core autophagy machinery (1, 6). Formation of phagophore is initiated by activation and translocation of ULK1 protein kinase from cytosol to the endoplasmic reticulum (7). This step is regulated by mammalian target of rapamycin (mTOR)[3] kinase, a cell growth regulator, which inhibits autophagy when nutrients are available in the cell, by phosphorylating ULK1. ULK1 is positively regulated by AMP-activated protein kinase (AMPK), an energy sensor (8). Activated ULK1 complex initiates autophagy by phosphorylating components of type III phosphatidylinositol 3-kinase complex, which contains VPS34 and Beclin1. Phosphorylated Beclin1 promotes generation of phosphatidylinositol 3-phosphate (PI3P) by VPS34, which recruits effectors such as DFCP1 and the WIPI (WD-repeat phosphoinositide interacting) family of proteins (9, 10). These proteins then recruit ATG12-5-16L1 complex and ATG3-LC3 conjugate to the phagophore (11). ATG5, which is conjugated to ATG12, interacts with ATG16L1 (12). ATG12-5-16L1 complex functions as E3 ligase in a ubiquitination-like reaction that conjugates LC3-I with phosphatidylethanolamine to produce LC3-II, which is membrane-associated. The LC3 family of proteins is needed for several functions such as expansion and closure of phagophore to form autophagosome, and recruitment of cargo (13, 14).

During formation of autophagosomes, the cargo that needs to be degraded is recruited to autophagosomes by specialized

This work was supported by Council of Scientific and Industrial Research, Government of India Grants BSC-0115 and BSC-0208 (to G. S.). G. S. is grateful to the Dept. of Science and Technology, Government of India for J C Bose National Fellowship Grant SR/S2/JCB-41/2010. M. Bansal and S. C. M are recipients of a Research Fellowship from the Council of Scientific and Industrial Research, New Delhi, India. The authors declare that they have no conflict of interest with the content of this article.

This article contains Figs. S1–S6.

[1] Present address: Department of Medicine, National Jewish Health, Denver, CO 80206

[2] To whom correspondence should be addressed: E-mail: gshyam@ccmb.res.in.

[3] The abbreviations used are: mTOR, mammalian target of rapamycin; AMPK, AMP-activated protein kinase; EBSS, Earle's balanced salt solution; LC3, microtubule-associated protein 1 light chain 3; LIR, LC3-interacting region; MEF, mouse embryonic fibroblast; NDP52, nuclear dot protein 52 kDa; NF-κB, nuclear factor κb; OPTN, human optineurin; Optn, mouse optineurin; PI3P, phosphatidylinositol 3-phosphate; UBD, ubiquitin-binding domain; UT, untreated.

proteins known as autophagy receptors such as optineurin (OPTN), p62, NDP52, NBR1, and TAXBP1 (2, 15–17). These autophagy receptors directly interact with the autophagosomal protein LC3 and ubiquitinated cargo through well-defined binding sites (2, 16, 18). OPTN is a cytoplasmic adaptor protein involved in mediating various cellular processes such as vesicle trafficking, signaling to transcription factors NF-κB and IRF3, and autophagy (16, 19–29). It is mainly a coiled coil protein with a ubiquitin-binding domain (UBD) and a zinc finger domain in the C-terminal region, and an LC3-interacting region in the N-terminal half of the protein (16, 19, 20). It has no catalytic activity and performs its diverse functions through interaction with various proteins (19, 20, 30–32). The function of OPTN as an autophagy receptor is important for clearance of cytosolic *Salmonella* and mutant proteins (Huntington, TDP43, SOD1) that form aggregates associated with neurodegenerative diseases (33, 34). Along with other autophagy receptors, OPTN mediates autophagy of damaged mitochondria (35–39). Although OPTN and NDP52 play a vital role in recruiting LC3 to damaged mitochondria, LC3-II production upon induction of mitophagy does not depend on these autophagy receptors (39). It has been shown that OPTN, along with other proteins, NDP52 and T6BP, plays a role in autophagosome maturation by linking myosin VI to autophagosomes (40).

Mutations in OPTN are associated with adult-onset primary open-angle glaucoma and amyotrophic lateral sclerosis (ALS) (41, 42). Although not mutated, OPTN is also associated with pathological structures seen in many neurodegenerative diseases (43). Glaucoma-associated mutants of OPTN are generally single copy missense mutations, whereas ALS-causing mutations include missense, deletion, and truncation mutations (31). A glaucoma-associated mutant of OPTN, E50K, inhibits autophagy that contributes to apoptotic death of retinal cells (44, 45). Transgenic mice expressing E50K-OPTN show mitochondrial fission, mitophagy, and degeneration of retinal ganglion cells (46). Another variant, M98K-OPTN, causes enhanced autophagy that also results in death of retinal cells (47). The ALS-associated mutant, E478G-OPTN, is impaired in mediating autophagic clearance of aggregated proteins, bacteria, and damaged mitochondria (33, 34, 48). Thus, impaired autophagy appears to play an important role in the pathogenesis caused by OPTN mutants. Therefore, it is essential to understand in detail the role of Optn in autophagy.

In this study, we have explored the role of Optn in autophagosome formation during basal and starvation-induced autophagy. Our results show that Optn deficiency leads to reduced LC3-II production and reduced formation of autophagosomes although the formation of phagophores (Wipi2-positive puncta) is not reduced. We have also investigated the role of Optn in the recruitment of Atg12-5-16L1 complex to Wipi2-positive phagophores. Our results suggest that Optn potentiates autophagosome formation by facilitating the recruitment of Atg12-5-16L1 complex to Wipi2-positive phagophore upstream of LC3-II production. We also show that an ALS-associated mutant, E478G-OPTN, is defective in autophagosome formation, and unlike optineurin, does not colocalize with Atg12-positive or Atg16L1-positive phagophores.

Results

Effect of Optn deficiency on basal and starvation-induced autophagy

Optn gene was inactivated by replacing ATG containing exon 2 with a cassette containing β-galactosidase reporter and neomycin resistance gene through homologous recombination (Fig. 1*A*). Disruption of *Optn* gene was confirmed by PCR and Southern blot using mouse tail DNA (Fig. 1, *B* and *C*). These mice were used to generate $Optn^{+/+}$ (wild type, WT) and $Optn^{-/-}$ (knock-out, KO) embryonic fibroblasts. Optn protein level was examined by Western blotting of $Optn^{-/-}$ and $Optn^{+/+}$ mouse embryonic fibroblast (MEF) extracts using an antibody that recognizes a C-terminal epitope of Optn. Optn band of about 67 kDa was seen in $Optn^{+/+}$ cells but it was not seen in $Optn^{-/-}$ MEFs (Fig. 1*D*).

To examine the contribution of Optn to basal and starvation-induced autophagy we used Optn knock-out MEFs. Upon induction of autophagy, cytosolic 18-kDa LC3-I form is lipidated to produce LC3-II form by Atg12-5-16L1 complex. The LC3-II form is crucial for the formation of autophagosomes, and the level of LC3-II form serves as an indicator of autophagy (49). Therefore, we examined the level of LC3b-II in wild type and Optn-deficient MEFs by Western blotting. The level of LC3b-II form was lower in $Optn^{-/-}$ MEFs when compared with $Optn^{+/+}$ MEFs (Fig. 1, *E* and *F*). Upon induction of autophagy the LC3-I is converted to LC3-II that is degraded through lysosomal pathway, which can be blocked by lysosomal inhibitors such as chloroquine. When autophagy was induced by starvation in presence of chloroquine, significantly lower level of LC3b-II was seen in $Optn^{-/-}$ MEFs compared with $Optn^{+/+}$ MEFs (Fig. 1, *E* and *F*). The reduced level of LC3b-II seen in Optn-deficient cells could be because of a reduction in LC3b mRNA level. Therefore, the level of LC3b mRNA was determined in these cells by quantitative PCR. The level of LC3b mRNA was not lower in $Optn^{-/-}$ MEFs compared with $Optn^{+/+}$ MEFs (Fig. 1*G*). Upon induction of autophagy by starvation for 2 h there was significant increase in LC3b mRNA level in $Optn^{+/+}$ MEFs but in $Optn^{-/-}$ MEFs there was only a marginal (statistically insignificant) increase (Fig. 1*G*). The starvation-induced increase in LC3b mRNA level in $Optn^{+/+}$ MEFs is possibly because of increase in its demand for protein synthesis due to higher level of autophagy.

Reduced formation of autophagosomes in $Optn^{-/-}$ MEFs

The reduced level of LC3-II form in $Optn^{-/-}$ cells indicated that autophagy is reduced in these cells. Therefore, we examined the number of autophagosomes (LC3b-positive dots) in the cells by staining endogenous LC3b. The number of autophagosomes was significantly reduced in $Optn^{-/-}$ MEFs compared with $Optn^{+/+}$ MEFs under basal condition as well as under condition of autophagy induction by amino acid starvation (Fig. 1, *H* and *I*). We also examined the formation of autophagosomes and autolysosomes by using a fluorescence reporter, mCherry-GFP-LC3B, which produces a fusion protein present in autophagosomes as well as autolysosomes but fluorescence of GFP is not visible in autolysosomes because of sensitivity of GFP fluorescence to low pH of autolysosomes

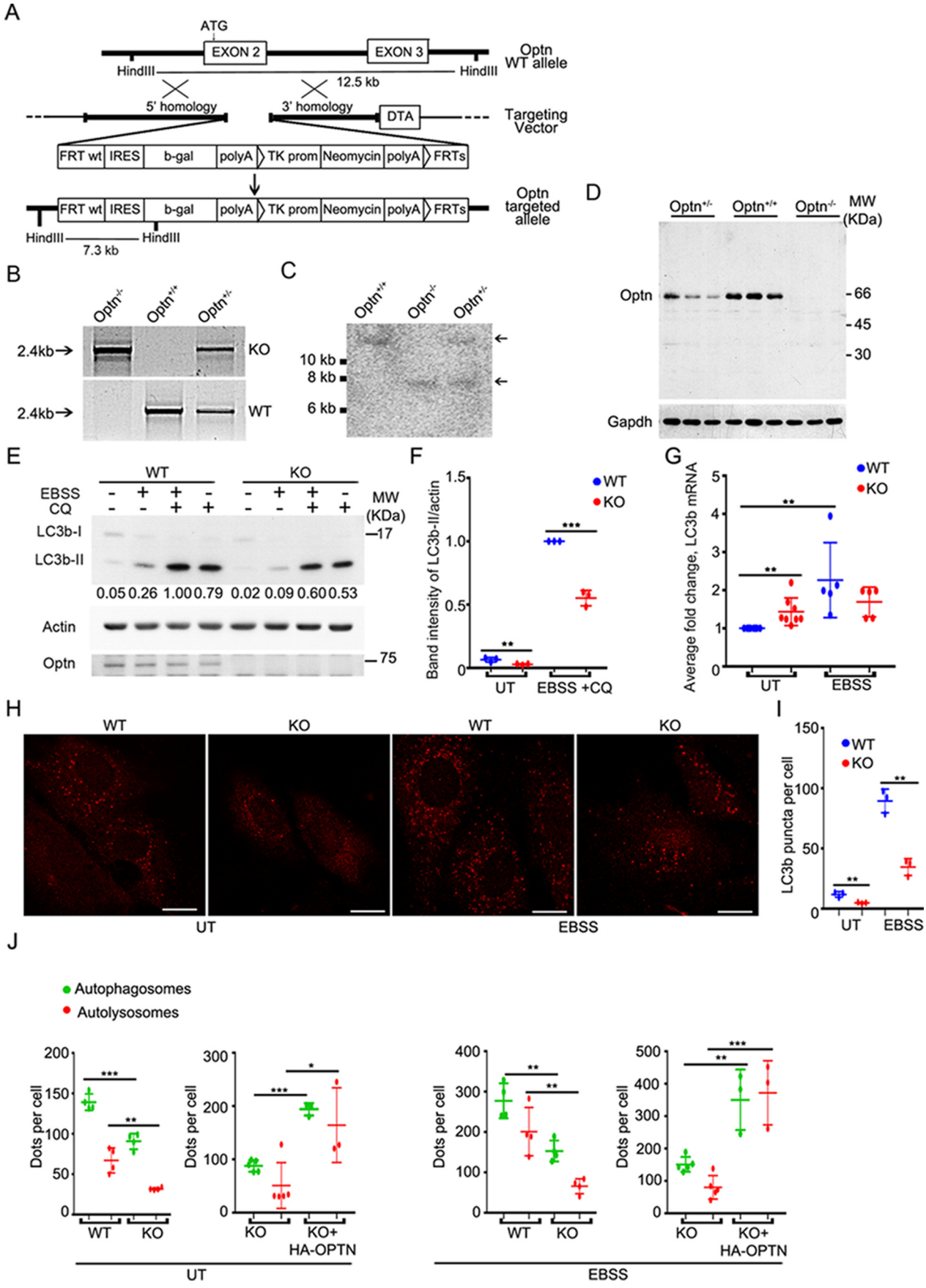
A
ATG
EXON 2
EXON 3
Optn WT allele
HindIII
12.5 kb
HindIII
5' homology
3' homology
DTA
Targeting Vector
FRT wt
IRES
b-gal
polyA
TK prom
Neomycin
polyA
FRTs
Optn targeted allele
HindIII
7.3 kb
HindIII
B
Optn-/-
Optn+/+
Optn+/-
2.4kb
KO
2.4kb
WT
C
Optn+/+
Optn-/-
Optn+/-
10 kb
8 kb
6 kb
D
Optn+/-
Optn+/+
Optn-/-
MW (KDa)
Optn
66
45
30
Gapdh
E
WT
KO
EBSS
CQ
MW (KDa)
LC3b-I
LC3b-II
17
0.05 0.26 1.00 0.79 0.02 0.09 0.60 0.53
Actin
Optn
75
F
Band intensity of LC3b-II/actin
WT
KO
UT
EBSS +CQ
G
Average fold change, LC3b mRNA
WT
KO
UT
EBSS
H
WT
KO
WT
KO
UT
EBSS
I
LC3b puncta per cell
WT
KO
UT
EBSS
J
Autophagosomes
Autolysosomes
Dots per cell
WT
KO
KO
KO+ HA-OPTN
UT
EBSS

(15). Plasmid expressing mCherry-GFP-LC3B was transfected in Optn$^{-/-}$ and Optn$^{+/+}$ MEFs and the number of autophagosomes and autolysosomes was analyzed by confocal microscopy. The number of autophagosomes was significantly less in Optn$^{-/-}$ MEFs compared with wild type MEFs under basal condition as well as under condition of autophagy induction by amino acid starvation (Fig. 1*J* and Fig. S1). The number of autolysosomes was also reduced in Optn$^{-/-}$ cells under both basal as well as starvation conditions. These defects in autophagosome and autolysosome formation were rescued by expression of wild type OPTN in Optn$^{-/-}$ MEFs (Fig. 1*J* and Fig. S1).

Formation of Wipi2-positive puncta is not reduced in Optn-deficient cells

To elucidate the role of Optn in autophagosome formation, we examined the effect of Optn deficiency on autophagy signaling by mTORC1 complex and AMPK. mTORC1 inhibits autophagy under conditions of nutrient sufficiency in part by phosphorylating Ulk1 at many residues including Ser-757. Optn$^{-/-}$ and Optn$^{+/+}$ MEFs did not show any significant difference in phosphorylation of mTORC1 kinase target S6K1 and Ser-757 residue of Ulk1, as determined by Western blotting (Fig. S2). However, despite being deficient in autophagy, Optn$^{-/-}$ MEFs showed higher level of phosphorylation of AMPK at Thr-172, a site involved in its activation (Fig. S3). The level of AMPK was similar in Optn$^{-/-}$ and Optn$^{+/+}$ MEFs (Fig. S3). Phosphorylation of AMPK target site Ser-555 of Ulk1 was also significantly higher in Optn$^{-/-}$ MEFs compared with Optn$^{+/+}$ cells (Fig. S3). Even the level of Ulk1 was significantly higher in Optn$^{-/-}$ MEFs (Fig. S3). These results suggest that reduced autophagy in Optn$^{-/-}$ MEFs is not likely to be because of altered mTORC1 or AMPK signaling. It is likely that in Optn$^{-/-}$ MEFs, reduced autophagy leads to activation of a feedback mechanism that results in AMPK activation, in an attempt by the cell to restore autophagy. However, despite activation of AMPK, Optn$^{-/-}$ cells are not able to restore normal level of autophagy because of a requirement of Optn at a later step involved in autophagosome formation.

Reduced formation of autophagosomes in Optn-deficient cells could be because of a requirement of Optn at an early stage of autophagosome biogenesis. In an hierarchical analysis of autophagosome formation site, it was shown that WIPI proteins, which are PI(3)P effector proteins, are recruited upstream of ATG12-5-16L1 and LC3 on the autophagosome formation site (50). Therefore, we next examined the number of phagophores in Optn-deficient cells by staining for endogenous Wipi2, which is present in these structures. The number of Wipi2-positive puncta was not reduced but increased in Optn-deficient MEFs compared with wild type MEFs (Fig. 2*A*). However, the level of Wipi2 protein was not higher in Optn$^{-/-}$ cells as determined by Western blotting (Fig. 2*D*). Treatment of cells with wortmannin, an inhibitor of PI3K, drastically reduced the number of Wipi2-positive puncta in Optn$^{+/+}$ as well as Optn$^{-/-}$ MEFs, suggesting that increased number of Wipi2-positive puncta in Optn$^{-/-}$ MEFs was not because of aggregate formation (Fig. S4). Upon induction of autophagy by starvation, there was an increase in the number of Wipi2-positive puncta in Optn$^{+/+}$ as well as Optn$^{-/-}$ MEFs but there was no significant difference in the number of Wipi2-positive puncta between Optn$^{+/+}$ and Optn$^{-/-}$ MEFs (Fig. 2*A*). These results suggest that Optn is not required for Wipi2-positive phagophore formation.

Atg16L1-positive puncta are reduced in Optn$^{-/-}$ cells

Increased number of Wipi2-positive puncta in Optn-deficient cells indicated that phagophores are formed, but these do not mature efficiently into autophagosomes because mature autophagosomes do not have Wipi2 (51). This suggested that Optn is required downstream of phagophore formation. During autophagosome biogenesis Wipi2 mediates recruitment of Atg12-5-16L1 complex to the phagophore, which is an essential step for conversion of LC3-I to LC3-II (11). Therefore, we determined the number of Atg16L1-positive puncta in Optn-deficient cells by staining for endogenous Atg16L1. The number of Atg16L1-positive puncta was significantly reduced in Optn-deficient MEFs compared with wild type MEFs under basal condition and also upon induction of autophagy by amino acid starvation (Fig. 2*B*). Reduced number of Atg16L1-positive puncta in Optn$^{-/-}$ cells was not because of lower level of Atg16L1 protein or Atg12-5 conjugate in these cells (Fig. 2*D*). We also determined the number of Atg12-positive puncta in these cells by staining for endogenous Atg12 and found that the number of Atg12-positive puncta was significantly lower in Optn$^{-/-}$ cells compared with wild type cells under basal condition and also upon induction of autophagy by starvation (Fig. 2*C*).

Optn facilitates recruitment of Atg16L1 to Wipi2-positive phagophores

Our results described so far showed that formation of LC3-II and the number of Atg16L1-positive puncta was reduced in Optn-deficient cells but the number of Wipi2-positive puncta was not reduced. This raised the possibility that recruitment of Atg12-5-16L1 complex to Wipi2-positive structures is

Figure 1. Optn$^{-/-}$ MEFs are deficient in autophagosome formation. *A*, strategy for generating Optn$^{-/-}$ MEFs. Exon 2 of optineurin was replaced with a selection cassette through homologous recombination. *B*, PCRs of mouse tail DNA showing optineurin knockout (KO) and wild type (WT) bands. *C*, Southern blot of mouse tail DNA showing 12.5-kb band of WT allele and 7.3 kb-band of knockout allele. *D*, Western blot showing absence of optineurin protein (67 kDa) in Optn$^{-/-}$ MEFs. *E*, Western blot showing LC3-II levels in Optn$^{+/+}$ (WT) and Optn$^{-/-}$ (KO) MEFs untreated or treated with EBSS (2 h) and/or chloroquine (50 μm, 2 h). Numbers below the blots indicate relative expression levels after normalization with actin, which was used as loading control. *F*, the graph represents comparison of LC3b-II protein levels normalized with actin (± S.D.), between WT and KO MEFs untreated (*UT*) or treated with EBSS and chloroquine for 2 h. $n = 3$ experiments; ***, $p < 0.001$; **, $p < 0.01$. *CQ*, chloroquine. *G*, graph showing comparison of average (± S.D.) of LC3b mRNA levels in WT and KO MEFs, untreated and treated with EBSS for 2 h. $n = 8$ for untreated and $n = 5$ for EBSS-treated samples; **, $p < 0.01$. *H*, LC3b staining in WT and KO MEFs, untreated or starved in EBSS for 2 h. Representative images are shown. *Scale bar*: 20 μm. *I*, graph represents average (± S.D.) number of LC3b puncta per cell. $n = 3$ experiments with minimum 50 cells in each experiment; **, $p < 0.01$ *versus* wild type. *J*, quantitation of number of autophagosomes and autolysosomes in WT and KO MEFs transfected with mCherry-GFP-LC3B construct with or without HA-OPTN, untreated or treated with EBSS for 2 h. $n = 4$ for WT MEF *versus* KO MEF graph (UT and EBSS treated). For KO MEF *versus* HA-OPTN graph, $n = 5$ for KO MEF and $n = 3$ for HA-OPTN MEF (UT and EBSS treated). Each *n* represents an experiment done with minimum 20 cells; ***, $p < 0.001$; **, $p < 0.01$; *, $p < 0.05$; scatter plots represent average ± S.D.

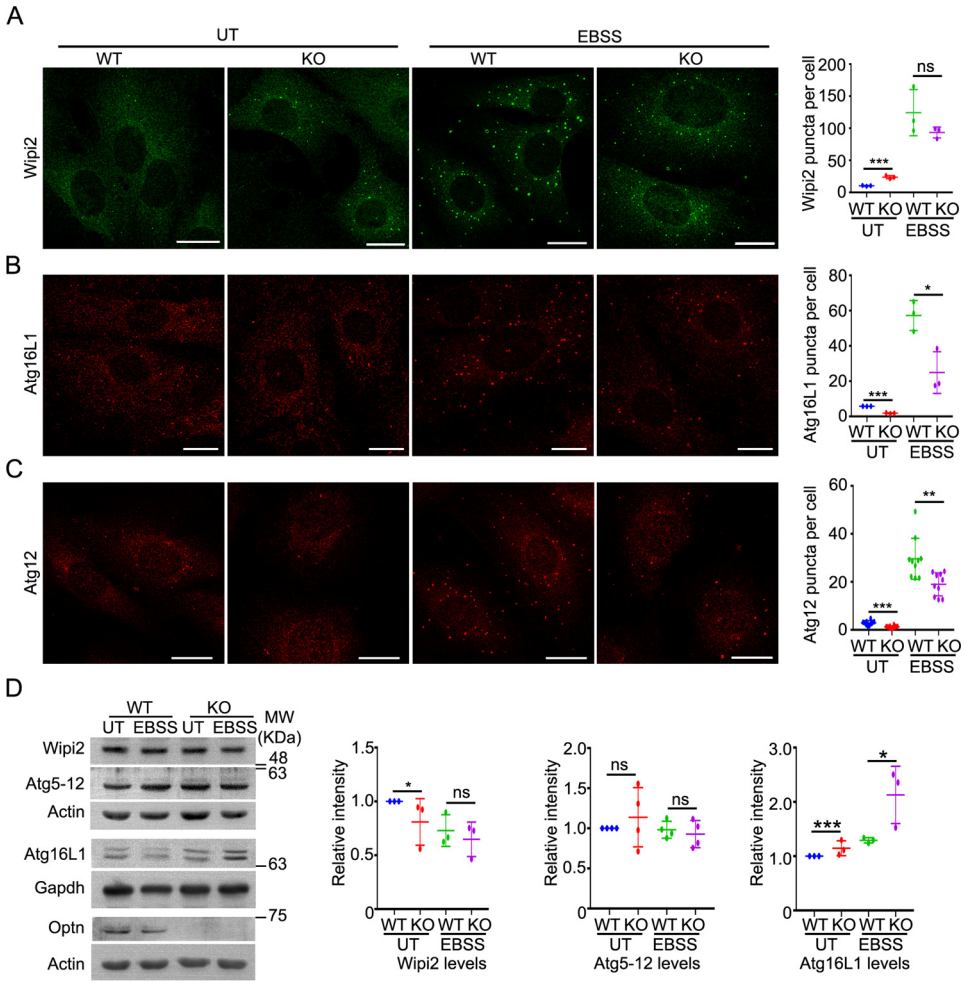

Figure 2. Wipi2-positive phagophore formation is not reduced in Optn$^{-/-}$ cells. *A–C*, WT and KO MEFs, untreated or treated with EBSS for 2 h and stained with either Wipi2 (*A*), Atg16L1 (*B*), or Atg12 (*C*), antibody. Quantitation of average (± S.D.) number of puncta per cell is shown in graph. $n = 3$ experiments with minimum 50 cells per experiment. ***, $p < 0.001$; **, $p < 0.01$; *, $p < 0.05$. *Scale bar*: 20 μm. *D*, Western blot showing levels of indicated proteins in WT and KO MEFs. Graphs represent average (± S.D.) amount of indicated protein from three experiments. *, $p < 0.05$; ***, $p < 0.001$.

impaired in Optn-deficient cells. We tested this hypothesis by examining the colocalization of endogenous Atg16L1 and Wipi2 in the puncta in Optn$^{+/+}$ and Optn$^{-/-}$ MEFs. The percentage of Wipi2-positive puncta that were also positive for Atg16L1 was significantly lower in Optn-deficient MEFs compared with wild type MEFs under basal condition and also upon induction of autophagy by starvation (Fig. 3, *A* and *B*). Induction of autophagy by starvation resulted in an increase in the percentage of Wipi2-positive puncta that were also positive for Atg16L1. Most of the Atg16L1-positive puncta were also positive for Wipi2 in wild type as well as Optn-deficient MEFs under condition of starvation (Fig. 3*B*). Next, we determined the percentage of Wipi2-positive puncta, that were also positive for Atg12, and found that these were significantly lower in Optn$^{-/-}$ cells compared with wild type cells under basal condition and also upon induction of autophagy by starvation (Fig. 3, *D* and *E*). These results suggest that Optn facilitates recruitment of Atg12-5-16L1 complex to Wipi2-positive phagophores. Most of the Atg12-positive puncta were also positive for Wipi2 in wild type as well as Optn-deficient cells under condition of starvation (Fig. 3*E*).

Optn deficiency affects the size of Atg16L1-positive vesicles

It has been shown that bigger size of Atg16L1 vesicles helps in LC3 incorporation into phagophore and autophagosome maturation (52). We estimated the size of Atg16L1-positive vesicles in Optn$^{+/+}$ and Optn$^{-/-}$ MEFs and observed that these vesicles were significantly smaller in size in Optn-deficient MEFs compared with wild type MEFs particularly upon autophagy induction by starvation (Fig. 3*C*). Induction of autophagy by starvation significantly increased the size of Atg16L1-positive vesicles in Optn$^{-/-}$ and Optn$^{+/+}$ cells (Fig. 3*C*). The size of Atg12-positive vesicles was also significantly smaller in Optn$^{-/-}$ MEFs compared with wild type MEFs (Fig. 3*F*). We next examined the ability of overexpressed wild type OPTN to enhance the formation of Atg16L1-positive puncta in Optn$^{-/-}$ MEFs cells by staining for endogenous Atg16L1. Expression of normal OPTN in the Optn-deficient resulted in a significant increase in the number as well as size of Atg16L1-positive puncta (Fig. 4, *A–C*). These results suggest that Optn deficiency affects the size of Atg16L1-positive vesicles in addition to the number of these vesicles.

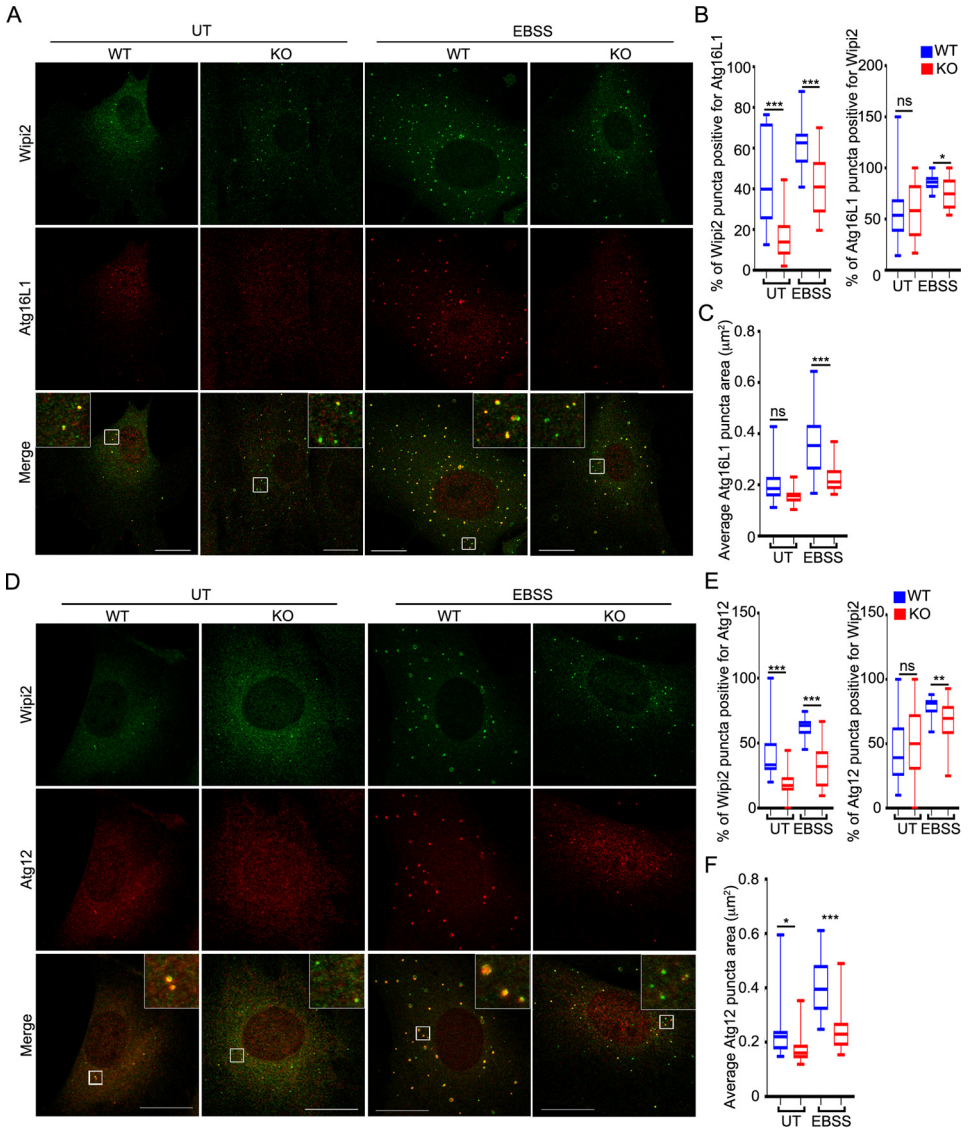

Figure 3. Optn$^{-/-}$ cells show reduced recruitment of Atg12-5-16L1 complex to Wipi2-positive phagophores. *A*, representative images showing WT and KO MEFs, untreated or treated with EBSS for 2 h and stained with Wipi2 and Atg16L1 antibodies. *Scale bar*: 20 μm. *B*, graphs showing percentage (average ± S.D.) of Wipi2 puncta positive for Atg16L1 and percentage of Atg16L1 puncta positive for Wipi2. ***, $p < 0.001$; *, $p < 0.05$. $n = 20$ cells. *C*, graph showing average (± S.D.) area of Atg16L1 puncta in WT and KO MEFs, untreated or treated with EBSS for 2 h. ***, $p < 0.001$. *D*, representative images showing WT and KO MEFs, untreated or treated with EBSS for 2 h, stained with Wipi2 and Atg12 antibodies. *Scale bar*: 20 μm. *E*, graphs showing percentage (average ± S.D.) of Wipi2 puncta positive for Atg12 and Atg12 puncta positive for Wipi2. ***, $p < 0.001$; **, $p < 0.01$. $n = 20$ cells. *F*, graph showing average area of Atg12 puncta in WT and KO MEFs, untreated or treated with EBSS for 2 h. ***, $p < 0.001$; *, $p < 0.05$. *Error bars*: mean ± S.D.

E478G-OPTN mutant is defective in autophagosome formation

One of the ALS-associated mutations of OPTN identified in the original study was E478G, which was suggested to be a disease-causing mutation (41, 53). This mutation is located in UBD of OPTN and it abolishes binding to ubiquitin (16). We confirmed that this mutant is defective in binding to polyubiquitin by GST pulldown assay using GST-Ub4 protein for pull down (Fig. S5). We examined its role in autophagy in Optn$^{-/-}$ MEFs by measuring the number of autophagosomes and autolysosomes. Optn$^{-/-}$ MEFs were transfected with mCherry-GFP-LC3B along with WT-OPTN or E478G-OPTN mutant or control plasmid. The number of autophagosomes as well as autolysosomes was significantly reduced in the cells expressing E478G-OPTN mutant, as compared with wild type OPTN-expressing cells under basal condition and also when autophagy was induced by amino acid starvation (Fig. 4, *D* and *E* and Fig. S6). The expression of wild type OPTN and E478G-OPTN mutant was comparable (Fig. 4*F*). We also examined the ability of wild type OPTN and its E478G mutant to enhance autophagosome formation in Optn$^{-/-}$ MEFs by staining for endogenous LC3b. Expression of normal OPTN in Optn-deficient cells resulted in a significant increase in the number of autophagosomes, whereas expression of E478G mutant did not show any increase (Fig. 4, *G* and *H*). Size of LC3-positive puncta in OPTN overexpressing cells was also significantly larger than nonexpressing cells, whereas E478G-OPTN overexpression did not show any significant difference (Fig. 4*I*). Overall, these results suggest that Optn promotes autophagosome formation during starvation-induced autophagy and the E478G-OPTN mutant is

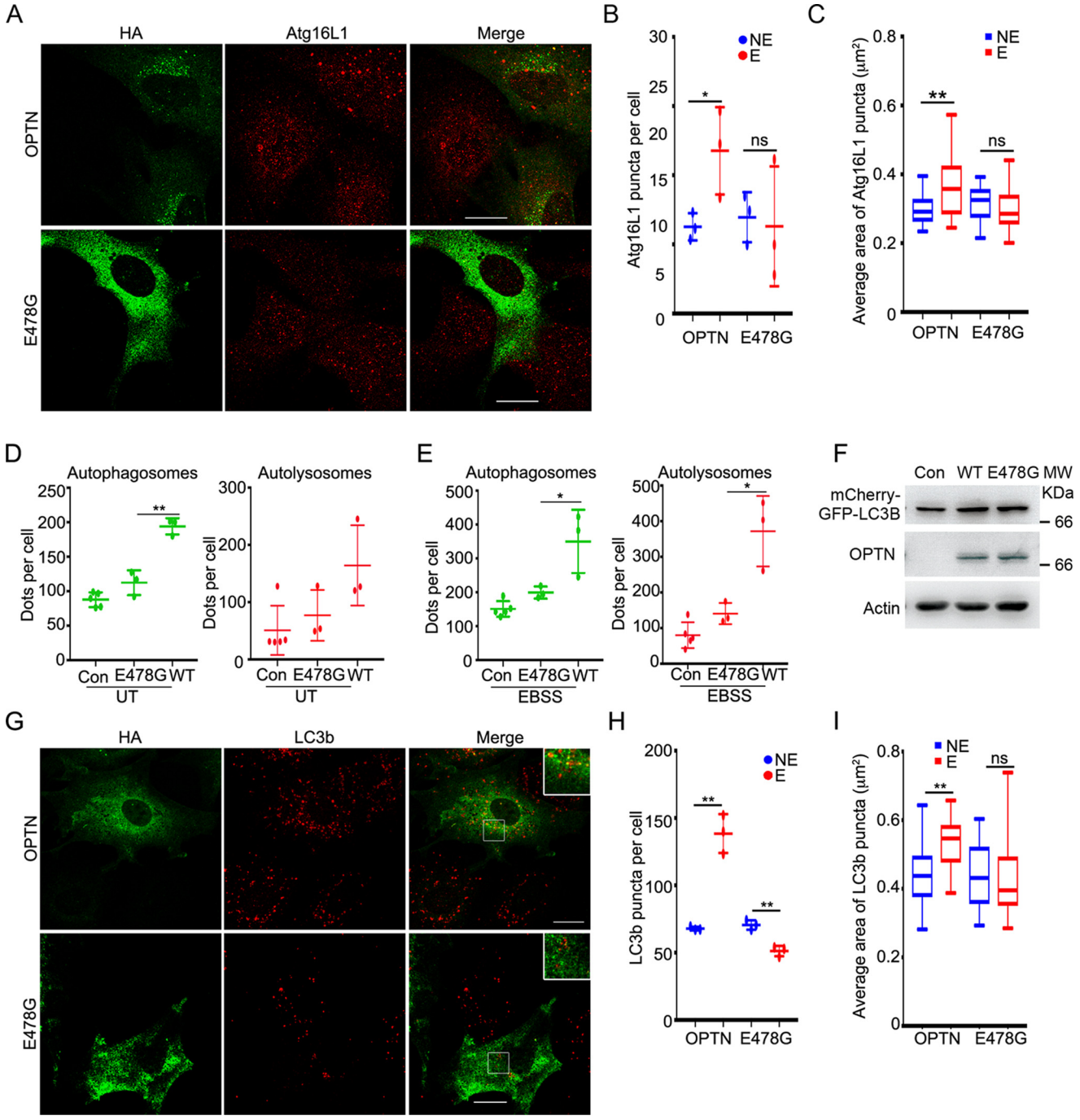

Figure 4. E478G mutant is defective in autophagosome formation. *A*, KO MEFs transfected with either HA-OPTN or HA-E478G were treated with EBSS for 2 h and stained for HA and Atg16L1. *Scale bar*: 20 μm. *B*, graphs show average (± S.D.) number of either Atg16L1 dots per cell in KO MEFs alone (nonexpressing, *NE*) or KO MEFs expressing HA-OPTN or HA-E478G and treated with EBSS for 2 h. $n = 3$ experiments with each experiment having minimum 20 expressing cells; *, $p < 0.05$. *C*, graphs showing average (± S.D.) area of Atg16L1 dots in KO MEFs alone (*NE*) or KO MEFs expressing HA-OPTN or HA-E478G and treated with EBSS for 2 h. **, $p < 0.01$; $n = 20$ cells. *D* and *E*, quantitation of number of autophagosomes and autolysosomes in KO MEFs transfected with mCherry-GFP-LC3B construct, along with control plasmid, HA-tagged OPTN or E478G mutant, untreated (*UT*) (*D*) or treated with EBSS for 2 h (*EBSS*) (*E*). $n = 3$ or more experiments with each experiment having minimum 20 cells; **, $p < 0.01$; *, $p < 0.05$. *F*, Western blot showing expression levels of mCherry-GFP-LC3B in Optn$^{-/-}$ MEFs transfected with mCherry-GFP-LC3B construct along with control plasmid, HA-tagged WT-OPTN or E478G mutant. *G*, KO MEFs transfected with either HA-OPTN or HA-E478G were treated with EBSS for 2 h and stained for HA and LC3b. *Scale bar*: 20 μm. *H*, graph shows average (± S.D.) number of either LC3b dots per cell in KO MEFs alone (nonexpressing, *NE*) or KO MEFs expressing HA-OPTN or HA-E478G (*E*) and treated with EBSS for 2 h. $n = 3$ experiments with each experiment having minimum 20 expressing cells, **, $p < 0.01$. *I*, graphs showing average (± S.D.) area of LC3b dots in KO MEFs alone (NE) or KO MEFs expressing HA-OPTN or HA-E478G and treated with EBSS for 2 h. **, $p < 0.01$; $n = 20$ cells.

defective in this function. We next examined the ability of the E478G-OPTN mutant to enhance the formation of Atg16L1-positive puncta in Optn$^{-/-}$ MEFs cells by staining for endogenous Atg16L1. Expression of E478G mutant did not show any increase in the number or size of Atg16L1-positive puncta (Fig. 4, *A–C*). These results suggest that the E478G mutation impairs the ability of OPTN to form Atg16L1-positive puncta as well as autophagosomes.

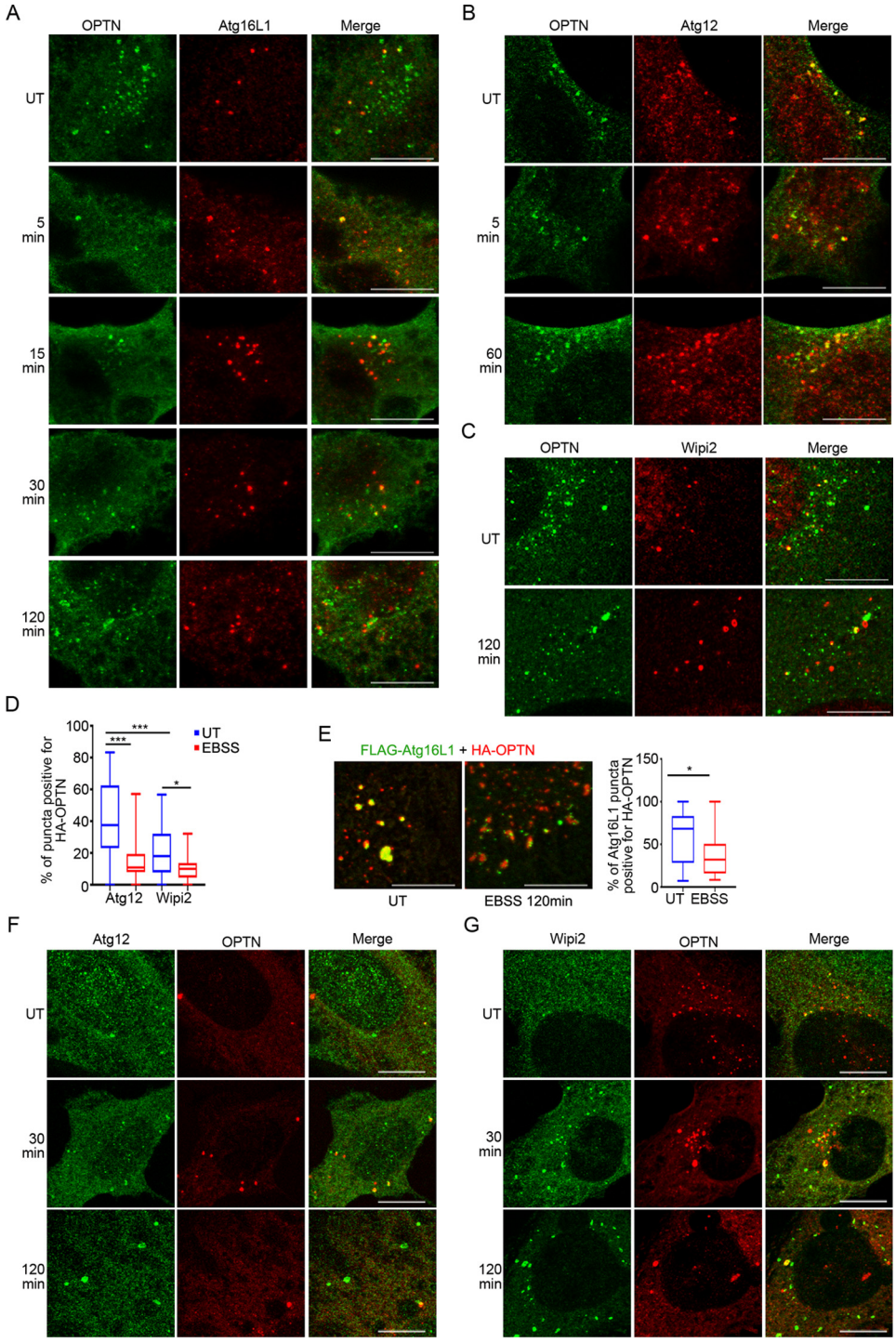

Figure 5. Optineurin is recruited to the phagophore. *A–C*, KO MEFs transfected with HA-OPTN were treated with EBSS for indicated time points and stained for HA and either Atg16L1 (*A*), or Atg12 (*B*), or Wipi2 (*C*). *Scale bar*: 10 μm. *D*, graph showing average (± S.D.) percentage of either Atg12 or Wipi2 puncta positive for HA-OPTN per cell in untreated or EBSS-treated KO MEFs. For Atg12 UT $n = 35$ and EBSS $n = 26$ cells. For Wipi2 UT $n = 27$, EBSS $n = 26$ cells. *E*, KO MEFs transfected with HA-OPTN and FLAG-Atg16L1, untreated or treated with EBSS for indicated time and stained for HA and FLAG. Graph shows average (± S.D.) percentage of FLAG-ATG16L1 puncta positive for HA-OPTN per cell in untreated or EBSS treated KO MEFs. $n = 20$ cells for UT and $n = 21$ cells for EBSS. *Scale bar*: 10 μm. *F* and *G*, MEFs stably expressing HA-Optn were treated with EBSS for indicated time points and stained for HA and either Atg12 (*F*) or Wipi2 (*G*). *Scale bar*: 10 μm. *UT*, untreated.

Recruitment of optineurin to the Atg12/16L1-positive puncta

Because Optn is involved in potentiating the recruitment of Atg12-5-16L1 complex to Wipi2-positive phagophore, it is likely to be recruited to these structures. Therefore, we overexpressed HA-OPTN in Optn$^{-/-}$ MEFs and examined the colocalization with endogenous Atg12, Atg16L1, and Wipi2 in the puncta (Fig. 5, *A–C*). OPTN showed good colocalization with Atg12-positive puncta, but colocalization with Wipi2-positive puncta was seen in much less percentage of puncta (Fig. 5*D*). Interestingly, upon induction of autophagy by starvation for

longer period, this colocalization of OPTN with all these three phagophore markers, Atg12, Atg16L1, as well as Wipi2, was considerably reduced and very few puncta showed colocalization (Fig. 5, *A–C*). Overexpressed FLAG-Atg16L1 showed robust colocalization with HA-OPTN in several puncta, which was reduced when cells were incubated in starvation medium for 120 min (Fig. 5*E*). Reduced colocalization of OPTN with Atg12/16L1-positive puncta upon induction of autophagy by starvation suggests that the recruitment of OPTN to these structures is transient. We also examined the recruitment of Optn to the phagophore in MEFs stably expressing HA-Optn, which were prepared by selection in G418. In these cells also, HA-Optn showed colocalization with Atg12 as well as Wipi2 in the puncta (Fig. 5, *F* and *G*). Induction of autophagy by starvation for short period (30 min) resulted in some increase in the number of Atg12 and Wipi2 puncta showing colocalization with stably expressed HA-Optn (Fig. 5, *F* and *G*). However, longer treatment with starvation medium resulted in reduced number of Atg12 and Wipi2 puncta showing colocalization with HA-Optn (Fig. 5, *F* and *G*). The results with stably expressing cells were essentially similar to those obtained with transiently overexpressed optineurin except that the colocalization was seen in lower number of puncta. These results provide further evidence for recruitment of Optn to the phagophore.

We used various mutants of OPTN to understand the mechanism of its recruitment to these pre-autophagosomal structures. The UBD mutant E478G did not show colocalization with endogenous Atg12-positive or Atg16L1-positive, or Wipi2-positive puncta (Fig. 6, *A–C*). The LC3-interacting region (LIR) mutant, F178A, like wild type OPTN, showed good colocalization with Atg12-positive puncta (Fig. 6*D*). These results suggest that the function of UBD is required for recruitment of OPTN to Atg12-positive puncta, but the function of LIR is not required.

Optn interacts with Atg5-12 conjugate

Because Optn is recruited to Atg12-5-16L1 complex, and facilitates recruitment of Atg12-5-16L1 complex to Wipi2-positive structures, it is likely that it formed a complex with one of the components of Atg12-5-16L1 complex and/or Wipi2. We tested this possibility by immunoprecipitation. GFP-OPTN or GFP was expressed in Optn$^{-/-}$ MEFs, and cell lysates were subjected to immunoprecipitation using GFP-Trap. The immunoprecipitates were then analyzed by Western blotting. GFP-OPTN but not GFP formed a complex with endogenous Atg5-12 conjugate and also with Wipi2 (Fig. 7*A*). Atg16L1 could not be seen in the GFP-OPTN immunoprecipitate, possibly because of weak reaction of this antibody in the Western blot. However, in HEK 293 cells, complex formation between GFP-OPTN and ATG5-12 conjugate, ATG16L1, and Wipi2 could be seen (Fig. 7*B*). Compared with wild type OPTN, the E478G mutant showed reduced formation of a complex with Atg12-5 conjugate and also with Wipi2 (Fig. 7*A*). Because E478G has a defective UBD, we tested the possibility of involvement of polyubiquitination in these interactions by comparing these interactions in presence or absence of deubiquitinase inhibitor, *N*-ethylmaleimide (NEM) in the immunoprecipitation buffer. But OPTN did not show weaker interaction with ATG5-12 or Wipi2 in absence of *N*-ethylmaleimide (Fig. 7*B*). We also examined the interaction of OPTN with Atg5 using GST pulldown assays and found that OPTN interacts with unconjugated HA-tagged Atg5 and also with Atg5-12 conjugate (Fig. 7*C*), whereas Wipi2 did not show any detectable interaction with GST-OPTN (Fig. 7*D*).

Ser-177 phosphorylation of OPTN promotes autophagosome formation

Phosphorylation of OPTN at Ser-177 is involved in the autophagic function of optineurin in clearance of bacteria, protein aggregates, and damaged mitochondria (16, 34, 35). Therefore, we investigated the requirement of Ser-177 phosphorylation of OPTN for autophagosome formation. The phospho-defective mutant S177A-OPTN, unlike normal OPTN or S177D-OPTN, did not enhance autophagosome formation in Optn-deficient cells, as determined by measuring the number of puncta formed by endogenous LC3b (Fig. 8*A*). Using mCherry-GFP-LC3B, we observed that the expression of S177A mutant in Optn-deficient cells resulted in reduced formation of autophagosomes (50.21 $\pm$ 31.73 S.D. in S177A, 92.82 $\pm$ 59.41 S.D. in WT-OPTN; p value 0.0002, $n = 39$ cells) and autolysosomes (31.36 $\pm$ 29.26 S.D. in S177A, 76.87 $\pm$ 65.76 S.D. in WT-OPTN; p value 0.0002, $n = 39$ cells) per cell, as compared with OPTN-expressing cells. Next, we examined the ability of S177A mutant to be recruited to Atg12-positive puncta by expressing it in Optn-deficient cells. This mutant, like wild type OPTN, showed good colocalization with Atg12-positive puncta (Fig. 8*B*). The phospho-mimic mutant, S177D-OPTN, also colocalized with Atg12-positive puncta (Fig. 8*B*), and like wild type OPTN, percentage of Atg12 puncta positive for S177D-OPTN (56.23% $\pm$ 6.13 S.E. in untreated (UT), 16.05 $\pm$ 5.28 S.E. in 60-min Earle's balanced salt solution (EBSS) treatment; p value 0.00002) decreased upon induction of autophagy by starvation. These results suggest that phosphorylation of OPTN at Ser-177 is required for autophagosome formation but not for its recruitment to Atg12-positive phagophore. We tested whether pSer-177–Optn is present in phagophores and found that it does colocalize with Wipi2-positive puncta (Fig. 8*C*).

Discussion

Our results show that Optn plays a role in basal as well as starvation-induced autophagy as seen by reduced LC3-II level, and reduced autophagosome and autolysosome number in Optn-deficient cells. This defect in autophagosome formation could be rescued by overexpressed OPTN, suggesting its direct involvement in this process. During autophagosome formation, the Atg12-5-16L1 complex is recruited to Wipi2-positive structure, and this step is a requirement for the conversion of LC3-I to LC3-II (11). LC3-II is associated with membrane and it is needed for expansion and closure of phagophore leading to formation of autophagosome. The results presented here suggest that Optn potentiates the recruitment of Atg12-5-16L1 complex to Wipi2-positive structures, and this function of Optn possibly contributes to autophagosome formation. This hypothesis is supported by our results showing that the forma-

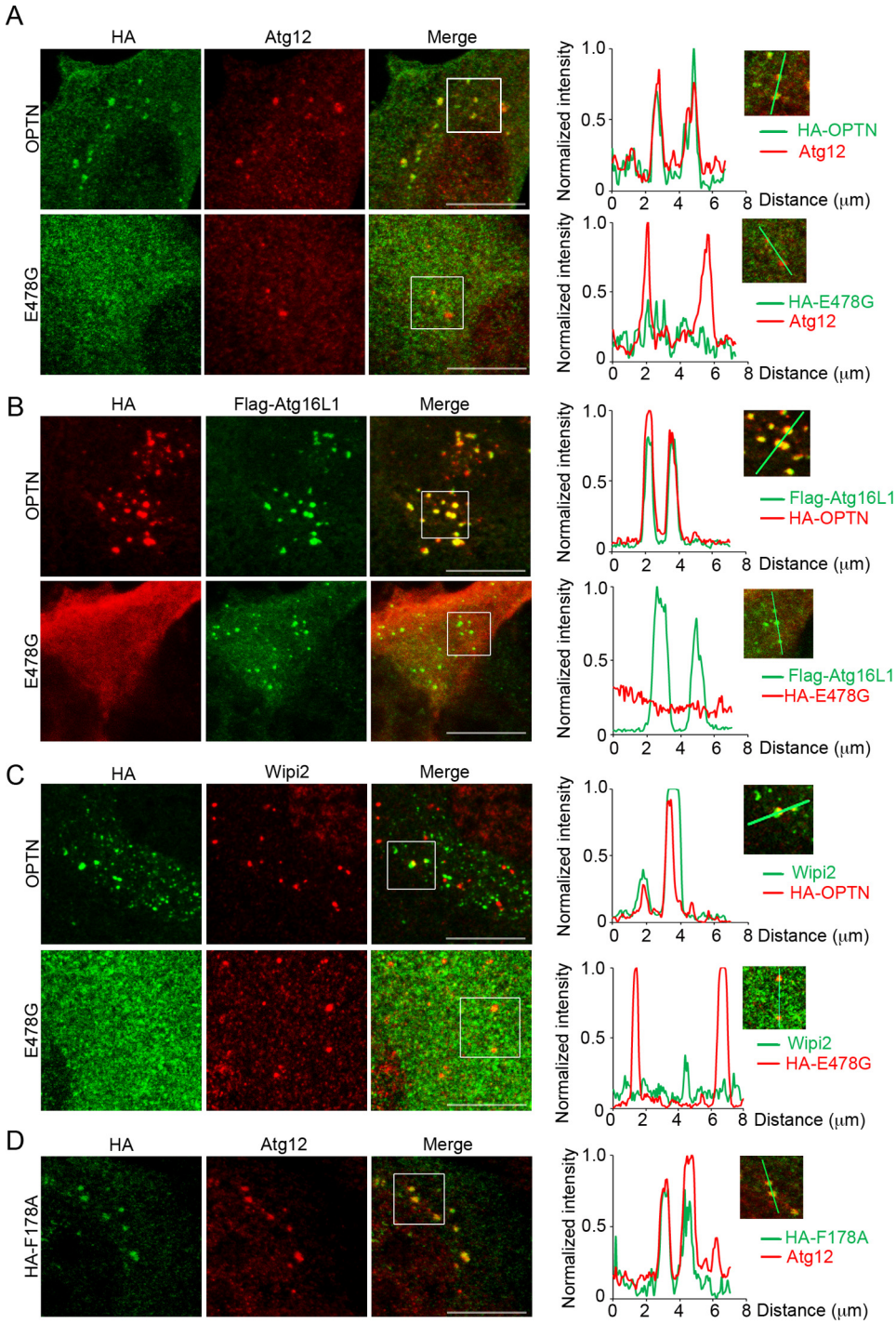

Figure 6. UBD but not LIR is required for recruitment of optineurin to the phagophore. *A*, KO MEFs transfected with either HA-OPTN or HA-E478G were stained for HA and Atg12. *Line scan* shows changes in OPTN or E478G intensity along Atg12 puncta; *Scale bar*: 10 μm. *B*, KO MEFs transfected with FLAG-Atg16L1 and either HA-OPTN or HA-E478G and stained for FLAG and HA. *Line scan* shows changes in OPTN or E478G intensity along Flag-Atg16L1 puncta. *Scale bar*: 10 μm. *C*, KO MEFs transfected with either HA-OPTN or HA-E478G were stained for HA and Wipi2. *Line scan* shows changes in OPTN or E478G intensity along Wipi2 puncta. *Scale bar*: 10 μm. *D*, KO MEFs transfected with HA-F178A were stained for HA and Atg12. *Line scan* shows changes in F178A intensity along Atg12 puncta; *Scale bar*: 10 μm.

tion of LC3-II, autophagosomes and Atg12/Atg16L1-positive puncta is reduced in Optn-deficient cells but formation of Wipi2-positive puncta is not reduced but increased. Interestingly Atg16L1-deficient MEFs, which are defective in autophagy, also show similar increase in Wipi2 puncta (11). Furthermore, the percentage of Wipi2-positive puncta, that are also positive for Atg16L1, is reduced in Optn-deficient MEFs compared with wild type MEFs. The size of Atg16L1 as well as LC3 puncta was also bigger in presence of Optn indicating toward the role of Optn in expansion of phagophore, which occurs during autophagosome formation.

Knockdown of Optn has been reported to induce accumulation of autophagosomes in NSC34 cells suggesting requirement of Optn for autophagosome-lysosome fusion (48). However, we

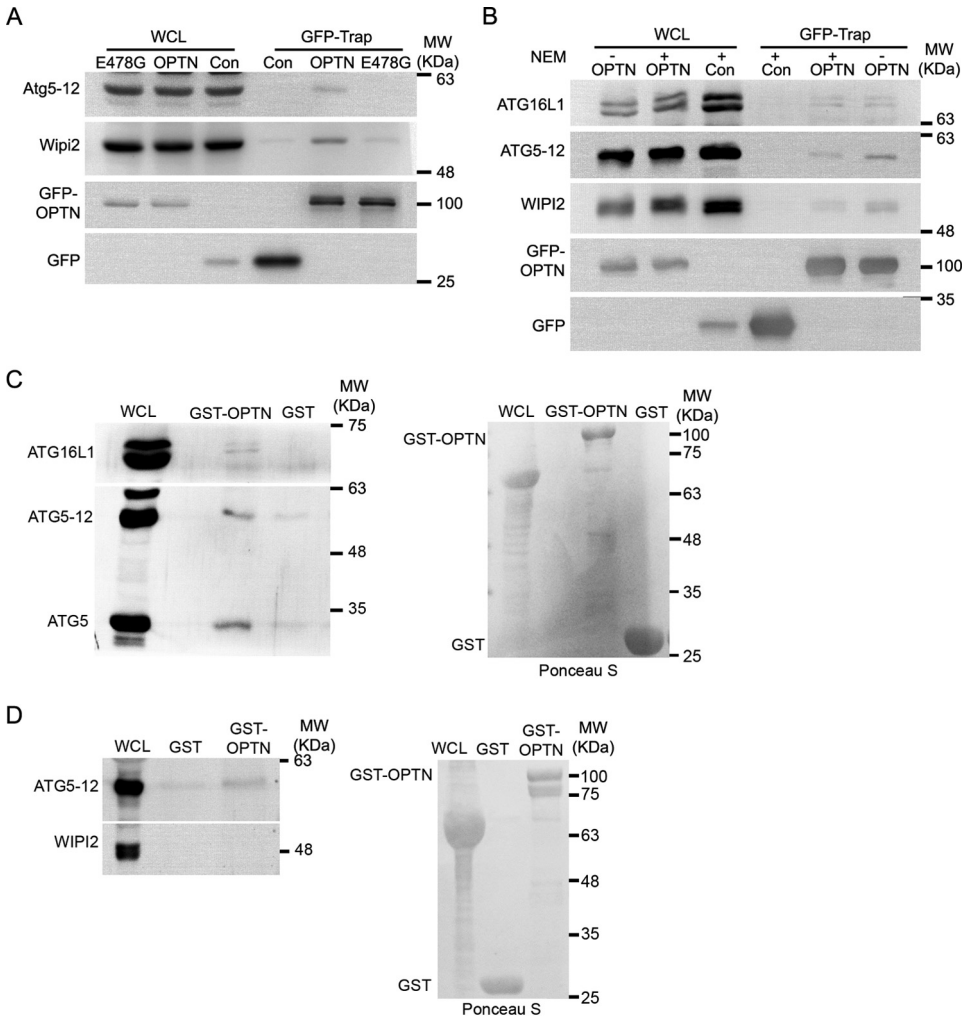

Figure 7. Optn forms a complex with Wipi2 and Atg5-12 conjugate. *A*, KO MEF cell lysates, expressing either GFP (*Con*), GFP-OPTN, or GFP-E478G were immunoprecipitated by GFP-Trap beads and subjected to Western blotting for indicated proteins. *B*, HEK 293 cell lysates, expressing either GFP alone (*Con*) or GFP-OPTN and subjected to immunoprecipitation by GFP-Trap beads, and immunoblotted for indicated proteins. *C*, optineurin tagged with GST or GST alone was immobilized on glutathione agarose beads and incubated with HEK cell lysates overexpressing HA-Atg5. Bound proteins were subjected to Western blotting for indicated proteins. *D*, optineurin tagged with GST or GST alone was immobilized on glutathione agarose beads and incubated with HEK cell lysates. Bound proteins were subjected to Western blotting for Wipi2 first and then Atg5.

did not observe accumulation of autophagosomes or LC3-II in Optn-deficient MEFs, indicating that some of the functions of Optn in autophagy may be cell type– dependent.

How does OPTN facilitate recruitment of Atg12-5-16L1 complex to Wipi2-positive structures? Recruitment of Optn into the Atg12/16L1-positive puncta and complex formation between Optn and Atg12-5 conjugate indicate that Optn is directly involved in this process. Atg16L1 is known to interact with Wipi2 directly and this interaction is important for recruitment of Atg12-5-16L1 complex to Wipi2-positive structures (11). However, this interaction is weak and we hypothesize that Optn facilitates recruitment of Atg12-5-16L1 complex to Wipi2-positive structures by forming a complex with the Atg12-5-16L1 conjugate. Some support for this hypothesis is provided by our observation that the functional UBD of Optn, which is required for autophagosome formation, is also required for its recruitment to the Atg12/16L1-positive phagophore, and for complex formation with Atg12-5 conjugate. Optn interacts with overexpressed unconjugated Atg5 and also with Atg12-5 conjugate, and this interaction of Optn may alter the conformation of Atg12-5-16L1 complex in such a way that leads to enhanced interaction with Wipi2 in the phagophore resulting in more efficient recruitment of Atg12-5-16L1 complex to the Wipi2-positive phagophore.

Structural studies have revealed that ATG12-5-16 complex consists of 2:2:2 stoichiometric complex of ATG12, ATG5, and ATG16L1, which has a unique six ubiquitin–fold architecture (54–57). ATG5 has two and ATG12 has one ubiquitin-fold. Interestingly, OPTN is a hexameric protein (20), which could conceivably bind with six ubiquitin-folds of ATG12-5-16L1 complex. However, this needs to be tested experimentally.

A recent study in yeast has shown interaction of yeast autophagy receptor Atg19 with Atg12-5-16 complex (58). Here it is shown that interaction of Atg19 with Atg5 stimulates Atg8 conjugation during selective autophagy in yeast. In this study interaction of OPTN with ATG5 is also shown but its significance in mammalian autophagy has not been explored.

Previous studies have focused on the role of OPTN in cargo selective autophagy of bacteria, damaged mitochondria, and mutant protein aggregates (16, 34, 35). Upon induction of

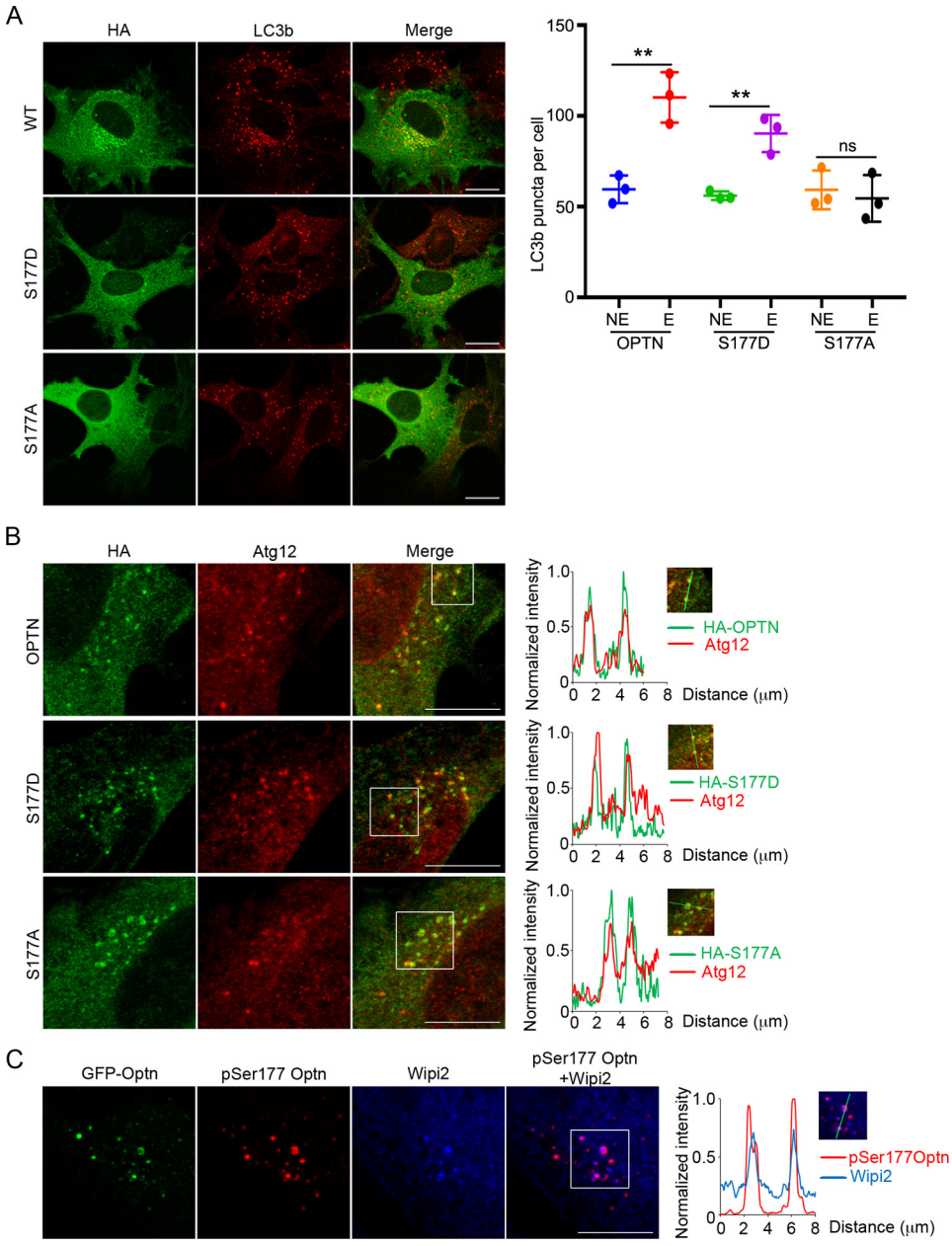

Figure 8. Ser-177 phosphorylation of optineurin promotes autophagosome formation, but it is not involved in recruitment to phagophore. *A*, KO MEFs transfected with either HA-OPTN or HA-S177A or HA-S177D were treated with EBSS for 2 h and stained for HA and LC3b. *Scale bar*: 20 μm. Graph shows average (± S.D.) number of LC3 dots per cell in KO MEFs alone (nonexpressing, *NE*) or KO MEFs expressing HA-OPTN or HA-S177A. $n = 3$ experiments, each experiment represents average of at least 20 expressing cells and nonexpressing cells. **, $p < 0.001$. *B*, KO MEFs transfected with either HA-OPTN or HA-S177D or HA-S177A were stained with HA and Atg12. *Line scan* indicates changes in intensity of HA tagged proteins along Atg12 puncta. *Scale bar*: 10 μm. *C*, confocal images of KO MEF expressing GFP-Optn and stained for pSer-177–Optn and Wipi2. *Line scan* indicates changes in intensity of pSer-177–Optn along Wipi2 puncta.

mitophagy by drugs that damage mitochondria, OPTN is recruited to damaged, ubiquitinated mitochondria through its UBD and mediates recruitment of various autophagy proteins upstream of LC3 (35, 39). OPTN and NDP52, which are recruited to damaged mitochondria with similar kinetics, have redundant functions in mitophagy upstream of LC3 recruitment to mitochondria (39). However, during mitophagy, production of LC3-II is not reduced when autophagy receptors including OPTN are knocked out (39). Our results show that Optn functions upstream of LC3-II production in nonselective autophagy to potentiate autophagosome formation. Thus, the precise functions of Optn in mitophagy and nonselective autophagy are different.

TBK1-mediated phosphorylation of OPTN at Ser-177 residue has been shown to enhance its LC3-binding and clearance of cytosolic *Salmonella* (16). This phosphorylation has also been found to be important for recruitment of LC3 to damaged mitochondria but not for recruitment of OPTN itself to damaged mitochondria (36). On the other hand UBD defective E478G mutant fails to localize to damaged mitochondria. In this study, we have found that Ser-177 phosphorylation is not required for recruitment of optineurin to

the Atg12-positive phagophores but it is required to form autophagosomes, whereas E478G mutant does not even colocalize with phagophores, indicating that optineurin has distinct roles during multistep process of autophagosome formation.

During autophagosome biogenesis membrane is needed that is provided by several organelles including endoplasmic reticulum, Golgi, plasma membrane, and recycling endosome (54). Atg16L1 is recruited from the cytosol into the endocytic vesicles at the plasma membrane and these vesicles traffic to recycling endosome before merging into forming autophagosome. Homotypic fusion of Atg16L1-positive vesicles enhances their size and delivery to forming autophagosome (52). Thus when Atg16L1 is recruited to Wipi2-positive structures, it is likely that during this process membrane is also delivered to these structures. By facilitating the recruitment of Atg16L1 complex to Wipi2-positive phagophore, Optn possibly also helps in the delivery of membrane during autophagosome formation. The mechanism involved in enhancing the number of Atg16L1-positive vesicles is not clear and will require further investigation. However, it is interesting to note that the E478G mutant is defective in restoring the number of Atg16L1-positive puncta in Optn-deficient cells.

In summary, our results show that Optn potentiates LC3-II production and maturation of phagophore into autophagosome during basal and starvation-induced autophagy. Our results also suggest that Optn, through its interaction with Atg5, facilitates the recruitment of Atg12-5-16L1 complex to the Wipi2-positive phagophore, and this function of Optn possibly mediates enhanced autophagosome formation. An ALS-associated mutant of OPTN, E478G, defective in ubiquitin binding, is also defective in autophagosome formation possibly because of impairment in its ability to be recruited to phagophore. Thus, we have identified a novel function of Optn in nonselective autophagy upstream of LC3-II production, which might have relevance to pathogenesis of ALS.

Materials and methods

Generation of Optn$^{-/-}$ mice and isolation of MEFs

Targeting vector containing neomycin resistance gene selection cassette flanked by *Optn* gene (NCBI Gene ID 71648) homology region adjacent to exon 2 and diphtheria toxin gene A (DTA) outside the homology region was electroporated in mouse 129S6/SvEvTac cross C57BL/6Ncr ES cell line (G4) (59). ES cells were maintained in DMEM supplemented with 10% fetal bovine serum, 0.1 mM minimum nonessential amino acids, 0.1 mM β-mercaptoethanol, 2 mM glutamax, 50 IU ml^{-1} penicillin, 50 μg ml^{-1} streptomycin, and 1000 units ml^{-1} leukemia inhibitory factor in a humidified incubator with 5% CO_2 at 37 °C. Electroporated ES cells were grown in G418 (250 μg ml^{-1}) containing selection medium for 10–14 days. G418-resistant ES cells were screened by PCR and homologous recombination was confirmed by Southern blotting. For identification of exon 2–deleted *Optn* allele by PCR, a forward primer was designed from neomycin cassette and the reverse primer was from exon 3 of *Optn* gene. To amplify wild type *Optn* allele, PCR primers were designed from the sequence of exon 2 (forward primer) and exon 3 (reverse primer). The size of PCR product was ~2.4 kb for both wild type and mutant *Optn* alleles. Mutant ES cells (10–12 cells) were injected into 3.5-day-old mouse blastocysts and these were transplanted into uterus of pseudopregnant CD-1 female. Chimeric males were crossed with CD-1 female to obtain germline transmission of mutant allele. Progeny was screened for mutated allele, and animals containing mutant allele were then interbred to get knock-out animals. Genotyping of mice was done by PCR of genomic DNA obtained from tail biopsy. The Institutional Animal Ethics Committee of the Centre for Cellular and Molecular Biology, India, approved all mice experiments. Animals were maintained in temperature, humidity, and light/dark controlled (12 h, 6 am–6 pm) environment and provided with autoclaved *ad libitum* diet.

MEFs were isolated from 13.5-day–post coitum embryos obtained from Optn$^{+/-}$ male female mating. Freshly collected embryos were placed in sterile phosphate-buffered saline (PBS). Head and inner organs were removed and used for genotyping. Remaining body was minced in DMEM, supplemented with 10% fetal bovine serum, using razor blade and seeded in T75 flask. MEFs were stored frozen in liquid nitrogen for future use.

Cell culture and transfection

MEFs and HEK 293T cells were maintained in DMEM supplemented with 10% fetal bovine serum in a humidified incubator with 5% CO_2 at 37 °C. DMEM for MEFs was supplemented with 0.1 mM β-mercaptoethanol, 50 IU ml^{-1} penicillin, and 50 μg ml^{-1} streptomycin. Transfections were performed using Lipofectamine 2000 (Invitrogen, 11669-019) or Lipofectamine (Invitrogen, 18324-012) and Lipofectamine with PLUS™ (Invitrogen, 11514-015) reagents according to manufacturer's instructions. For inducing starvation, cells were incubated in EBSS (Invitrogen, 14155063) containing $CaCl_2$ (1.8 mM) and $MgSO_4$ (0.81 mM) at 37 °C for indicated time after washing them three times with PBS. Cell lines were routinely stained with DAPI and checked for mycoplasma contamination.

Expression vectors

Plasmids expressing HA and GFP tagged human OPTN, its mutant HA-F178A, HA-S177A, HA-Atg5, and GST-OPTN have been described earlier (23, 27, 47, 60, 61). HA-E478G and HA-S177D mutants of OPTN were made by site-directed mutagenesis of HA-OPTN. Mouse Optn was amplified by RT-PCR and cloned into pEGFP-C3 vector. FLAG-Atg16L1 construct was kindly provided by Dr. Sharon Tooze (The Francis Crick Institute, London UK) (11). mCherry-GFP-LC3B construct was kindly provided by Dr. Terje Johansen (University of Tromsø, Tromsø, Norway) (15).

Antibodies and reagents

Rabbit polyclonal antibodies against the following proteins were used: optineurin (Abcam, ab23666; 1:1000 Western blotting (WB)), LC3B (Cell Signaling Technology (CST), 27755; 1:100 immunofluorescence (IF)), WIPI2 (Sigma, HPA019852; 1:2000 WB, 1:400 IF), Atg12 (Abcam, ab155589; 1:400 IF), HA

(Santa Cruz Biotechnology, sc-805; 1:1000 WB, 1:300 IF), GFP (Santa Cruz Biotechnology, sc-9996; 1:1000 WB), and ATG5 (CST, 8540; 1:1000 WB). Rabbit monoclonal antibodies used were Atg16L1 (CST, 8089; 1:1000 WB, 1:100 IF), AMPKα (CST, 5832; 1:1000 WB), phospho-AMPKα (Thr-172) (CST, 2535; 1:1000 WB), phospho-ULK1 (Ser-555) (CST, 5869; 1:1000 WB), phospho-ULK1 (Ser-757) (CST, 6888; 1:1000 WB), FLAG (Sigma, F-7425; 1:400 IF), and ULK1 (CST, 8054; 1:1000). pSer-177–OPTN antibody was a generous gift from Dr. Ivan Dikic of Goethe University Medical School (16). Mouse monoclonal antibodies used were LC3B (Enzo Life Sciences, ALX80308; 1:750 WB), HA (Roche Applied Biosystems, 11583816001; 1:400 IF, 1:1000 WB), WIPI2 (Abcam, ab105459; 1:1200 IF), GAPDH (Millipore, MAB374; 1:10000 WB), and Actin (Millipore, MAB1501; 1:10000 WB). Secondary antibodies used were Cy-3–conjugated anti-rabbit IgG (Amersham Biosciences, PA43004, 1:1500), HRP-conjugated anti-mouse IgG (Amersham Biosciences, NA9310; 1:6000), anti-rabbit IgG, HRP-linked antibody (CST, 7074; 1:2000), HRP conjugated anti-rabbit IgG (Amersham Biosciences, NA934; 1:8000), Alexa Fluor 633 anti-mouse IgG (Molecular Probes, A21050; 1:500), Alexa Fluor 633 anti-rabbit IgG (Molecular Probes, A21070; 1:500), Alexa Fluor 488 anti-rabbit IgG (Molecular Probes, A21206; 1:500). Chloroquine (Sigma, C6628) and wortmannin (Calbiochem, 681675) are commercially available.

Immunofluorescence microscopy

Cells were grown as monolayer on glass coverslip and transfected with required expression vectors. These cells were fixed in 3.7% formaldehyde, permeabilized using 0.5% Triton X-100 and 0.05% Tween 20, and incubated for 1 h with 2% BSA in PBS followed by incubation with primary antibody (47). For endogenous LC3 staining, cells were fixed with 3% paraformaldehyde for 20 min, followed by aldehyde quenching with 50 mM NH_4Cl for 10 min (51). Cells were permeabilized for 5 min with methanol at room temperature and blocked with 5% BSA for 1 h. Primary antibody diluted in 1% BSA was added and cells were incubated overnight at 4 °C. Appropriate secondary fluorescent antibody was used to visualize primary antibody binding. Mounting medium with DAPI was used to visualize the nucleus. The images were taken on LSM510 meta NLO confocal microscope from Carl Zeiss (Jena, Germany) or Leica TCS SP8 at 63X/1.4NA oil immersion objective lens. Line scans representing variation in intensity of the fluorophore across the line of interest were generated using LAS software (LAS X version 2.0.2.15022).

Autophagic flux measurement

Autophagic flux was measured by transfecting mCherry-GFP-LC3B construct in MEFs. Transfected cells were scanned using LSM510 meta NLO confocal microscope from Carl Zeiss (Jena, Germany) or Leica TCS SP8 using 63× oil immersion objective lens (NA 1.4). Optical Z-sections of 0.3-μm thickness of the cell were taken. Images were then analyzed using Imaris software (Bitplane, Switzerland) for counting the number of green and red dots. Dots that had both green and red fluorescence were taken as autophagosomes; only red dots (counted by subtracting green dots from total red dots) were counted as autolysosomes.

Puncta quantification

Number and size of puncta were quantified using ImageJ software. Optical Z sections of 0.35-μm thickness of the cell were taken using confocal microscope with 63× oil immersion objective lens. Puncta with area of 0.1–3.0 μm^2 were quantitated. To calculate double-positive puncta, those puncta that overlapped by at least 0.1 μm^2 of area were counted.

GFP-Trap, GST pulldown assay, and Western blotting

For immunoprecipitation using GFP-Trap, cells were transfected with plasmids expressing either empty GFP or GFP-tagged proteins for 20 h, washed with PBS, and lysed with buffer containing 10 mM Tris, 150 mM NaCl, 0.5 mM EDTA, 10 mM NaF, 2 mM Na_3VO_4, 10 mM *N*-ethylmaleimide, protease inhibitor mixture, and 0.5% Nonidet P-40. Lysates were clarified by centrifuging at 20,000 *g*, diluted to 0.2% Nonidet P-40, and incubated with GFP-Trap beads (ChromoTek) for 2 h at 4 °C. Beads were then washed three times, boiled in SDS sample buffer, and analyzed by Western blotting. For GST pulldown assays, GST and GST fusion proteins were expressed in *Escherichia coli* and immobilized on glutathione agarose beads (Sigma, G4510). These beads were incubated for 4 h with HEK 293T cell lysates expressing indicated proteins. After washing these beads three times, the bound proteins were eluted by boiling in SDS sample buffer and analyzed by Western blotting.

MEFs were washed three times with 1× PBS prior to lysing with SDS sample buffer. Lysates were boiled for 5–10 min, and resolved in SDS-PAGE. Proteins were transferred to PVDF or nitrocellulose membrane for Western blot analysis according to standard protocols described earlier (47).

Quantitative PCR

Total RNA from MEFs was isolated using TRIzol reagent (Invitrogen). cDNA synthesis was done by using SuperScript III First-Strand Synthesis System (Invitrogen) after DNase I (New England Biolabs) treatment. Quantitative PCR was done in 7900HT Fast Real-Time PCR System (Applied Biosystems). Expression of gene of interest was normalized with actin mRNA.

Statistical analysis

Scatter plots or box whisker plots represent average ± S.D. Statistical significance between averages was calculated using Student's *t* test (two-tailed). *p* value of less than 0.05 was considered significant.

Author contributions—M. Bansal planned, performed, and analyzed most of the experiments and wrote the manuscript. S. C. M. performed and analyzed some of the experiments in Figs. 1, 2, and 5. K. S. helped in performing experiment in Figs. 6*D* and 7*C*. C. S. performed experiment in Fig. S5. S. P. S., D. P. S., B. J. L., M. Buono, and S. K. contributed in performing experiments in Fig. 1, *A–D*. G. S. planned the experiments, analyzed the data, and wrote the manuscript. G. S. conceived and obtained funding for this study. All authors approved the final version of the manuscript.

Acknowledgments—We thank Drs. Terje Johansen, Ivan Dikic, and Sharon Tooze for providing reagents.

References

1. Yang, Z., and Klionsky, D. J. (2009) An overview of the molecular mechanism of autophagy. *Curr. Top. Microbiol. Immunol.* **335,** 1–32 Medline
2. Stolz, A., Ernst, A., and Dikic, I. (2014) Cargo recognition and trafficking in selective autophagy. *Nat. Cell Biol.* **16,** 495–501 CrossRef Medline
3. Levine, B., Packer, M., and Codogno, P. (2015) Development of autophagy inducers in clinical medicine. *J. Clin. Invest.* **125,** 14–24 CrossRef Medline
4. Nakamura, S., and Yoshimori, T. (2017) New insights into autophagosome-lysosome fusion. *J. Cell Sci.* **130,** 1209–1216 CrossRef Medline
5. Ktistakis, N. T., and Tooze, S. A. (2016) Digesting the expanding mechanisms of autophagy. *Trends Cell Biol.* **26,** 624–635 CrossRef Medline
6. Mizushima, N., Yoshimori, T., and Ohsumi, Y. (2011) The role of Atg proteins in autophagosome formation. *Annu. Rev. Cell Dev. Biol.* **27,** 107–132 CrossRef Medline
7. Mizushima, N. (2010) The role of the Atg1/ULK1 complex in autophagy regulation. *Curr. Opin. Cell Biol.* **22,** 132–139 CrossRef Medline
8. Kim, J., Kundu, M., Viollet, B., and Guan, K. L. (2011) AMPK and mTOR regulate autophagy through direct phosphorylation of Ulk1. *Nat. Cell Biol.* **13,** 132–141 CrossRef Medline
9. Axe, E. L., Walker, S. A., Manifava, M., Chandra, P., Roderick, H. L., Habermann, A., Griffiths, G., and Ktistakis, N. T. (2008) Autophagosome formation from membrane compartments enriched in phosphatidylinositol 3-phosphate and dynamically connected to the endoplasmic reticulum. *J. Cell Biol.* **182,** 685–701 CrossRef Medline
10. Polson, H. E., de Lartigue, J., Rigden, D. J., Reedijk, M., Urbé, S., Clague, M. J., and Tooze, S. A. (2010) Mammalian Atg18 (WIPI2) localizes to omegasome-anchored phagophores and positively regulates LC3 lipidation. *Autophagy* **6,** 506–522 CrossRef Medline
11. Dooley, H. C., Razi, M., Polson, H. E., Girardin, S. E., Wilson, M. I., and Tooze, S. A. (2014) WIPI2 links LC3 conjugation with PI3P, autophagosome formation, and pathogen clearance by recruiting Atg12-5-16L1. *Mol. Cell* **55,** 238–252 CrossRef Medline
12. Sakoh-Nakatogawa, M., Matoba, K., Asai, E., Kirisako, H., Ishii, J., Noda, N. N., Inagaki, F., Nakatogawa, H., and Ohsumi, Y. (2013) Atg12-Atg5 conjugate enhances E2 activity of Atg3 by rearranging its catalytic site. *Nat. Struct. Mol. Biol.* **20,** 433–439 CrossRef Medline
13. Nakatogawa, H., Ichimura, Y., and Ohsumi, Y. (2007) Atg8, a ubiquitin-like protein required for autophagosome formation, mediates membrane tethering and hemifusion. *Cell* **130,** 165–178 CrossRef Medline
14. Slobodkin, M. R., and Elazar, Z. (2013) The Atg8 family: Multifunctional ubiquitin-like key regulators of autophagy. *Essays Biochem.* **55,** 51–64 CrossRef Medline
15. Pankiv, S., Clausen, T. H., Lamark, T., Brech, A., Bruun, J. A., Outzen, H., Øvervatn, A., Bjørkøy, G., and Johansen, T. (2007) p62/SQSTM1 binds directly to Atg8/LC3 to facilitate degradation of ubiquitinated protein aggregates by autophagy. *J. Biol. Chem.* **282,** 24131–24145 CrossRef Medline
16. Wild, P., Farhan, H., McEwan, D. G., Wagner, S., Rogov, V. V., Brady, N. R., Richter, B., Korac, J., Waidmann, O., Choudhary, C., Dötsch, V., Bumann, D., and Dikic, I. (2011) Phosphorylation of the autophagy receptor optineurin restricts *Salmonella* growth. *Science* **333,** 228–233 CrossRef Medline
17. von Muhlinen, N., Thurston, T., Ryzhakov, G., Bloor, S., and Randow, F. (2010) NDP52, a novel autophagy receptor for ubiquitin-decorated cytosolic bacteria. *Autophagy* **6,** 288–289 CrossRef Medline
18. Lamark, T., Kirkin, V., Dikic, I., and Johansen, T. (2009) NBR1 and p62 as cargo receptors for selective autophagy of ubiquitinated targets. *Cell Cycle* **8,** 1986–1990 CrossRef Medline
19. Kachaner, D., Génin, P., Laplantine, E., and Weil, R. (2012) Toward an integrative view of Optineurin functions. *Cell Cycle* **11,** 2808–2818 CrossRef Medline
20. Ying, H., and Yue, B. Y. (2012) Cellular and molecular biology of optineurin. *Int. Rev. Cell Mol. Biol.* **294,** 223–258 CrossRef Medline
21. Hattula, K., and Peränen, J. (2000) FIP-2, a coiled-coil protein, links Huntingtin to Rab8 and modulates cellular morphogenesis. *Curr. Biol.* **10,** 1603–1606 CrossRef Medline
22. Zhu, G., Wu, C. J., Zhao, Y., and Ashwell, J. D. (2007) Optineurin negatively regulates TNFα-induced NF-κB activation by competing with NEMO for ubiquitinated RIP. *Curr. Biol.* **17,** 1438–1443 CrossRef Medline
23. Nagabhushana, A., Chalasani, M. L., Jain, N., Radha, V., Rangaraj, N., Balasubramanian, D., and Swarup, G. (2010) Regulation of endocytic trafficking of transferrin receptor by optineurin and its impairment by a glaucoma-associated mutant. *BMC Cell Biol.* **11,** 4 CrossRef Medline
24. Park, B., Ying, H., Shen, X., Park, J. S., Qiu, Y., Shyam, R., and Yue, B. Y. (2010) Impairment of protein trafficking upon overexpression and mutation of optineurin. *PLoS One* **5,** e11547 CrossRef Medline
25. Mankouri, J., Fragkoudis, R., Richards, K. H., Wetherill, L. F., Harris, M., Kohl, A., Elliott, R. M., and Macdonald, A. (2010) Optineurin negatively regulates the induction of IFNβ in response to RNA virus infection. *PLoS Pathog.* **6,** e1000778 CrossRef Medline
26. Gleason, C. E., Ordureau, A., Gourlay, R., Arthur, J. S., and Cohen, P. (2011) Polyubiquitin binding to optineurin is required for optimal activation of TANK-binding kinase 1 and production of interferon β. *J. Biol. Chem.* **286,** 35663–35674 CrossRef Medline
27. Nagabhushana, A., Bansal, M., and Swarup, G. (2011) Optineurin is required for CYLD-dependent inhibition of TNFα-induced NF-κB activation. *PLoS One* **6,** e17477 CrossRef Medline
28. Vaibhava, V., Nagabhushana, A., Chalasani, M. L., Sudhakar, C., Kumari, A., and Swarup, G. (2012) Optineurin mediates a negative regulation of Rab8 by the GTPase-activating protein TBC1D17. *J. Cell Sci.* **125,** 5026–5039 CrossRef Medline
29. Sahlender, D. A., Roberts, R. C., Arden, S. D., Spudich, G., Taylor, M. J., Luzio, J. P., Kendrick-Jones, J., and Buss, F. (2005) Optineurin links myosin VI to the Golgi complex and is involved in Golgi organization and exocytosis. *J. Cell Biol.* **169,** 285–295 CrossRef Medline
30. Chalasani, M. L., Swarup, G., and Balasubramanian, D. (2009) Optineurin and its mutants: Molecules associated with some forms of glaucoma. *Ophthalmic Res.* **42,** 176–184 CrossRef Medline
31. Bansal, M., Swarup, G., and Balasubramanian, D. (2015) Functional analysis of optineurin and some of its disease-associated mutants. *IUBMB Life* **67,** 120–128 CrossRef Medline
32. Minegishi, Y., Nakayama, M., Iejima, D., Kawase, K., and Iwata, T. (2016) Significance of optineurin mutations in glaucoma and other diseases. *Prog. Retin. Eye Res.* **55,** 149–181 CrossRef Medline
33. Shen, W. C., Li, H. Y., Chen, G. C., Chern, Y., and Tu, P. H. (2015) Mutations in the ubiquitin-binding domain of OPTN/optineurin interfere with autophagy-mediated degradation of misfolded proteins by a dominant-negative mechanism. *Autophagy* **11,** 685–700 CrossRef Medline
34. Korac, J., Schaeffer, V., Kovacevic, I., Clement, A. M., Jungblut, B., Behl, C., Terzic, J., and Dikic, I. (2013) Ubiquitin-independent function of optineurin in autophagic clearance of protein aggregates. *J. Cell Sci.* **126,** 580–592 CrossRef Medline
35. Wong, Y. C., and Holzbaur, E. L. (2014) Optineurin is an autophagy receptor for damaged mitochondria in parkin-mediated mitophagy that is disrupted by an ALS-linked mutation. *Proc. Natl. Acad. Sci. U.S.A.* **111,** E4439–E4448 CrossRef Medline
36. Moore, A. S., and Holzbaur, E. L. (2016) Dynamic recruitment and activation of ALS-associated TBK1 with its target optineurin are required for efficient mitophagy. *Proc. Natl. Acad. Sci. U.S.A.* **113,** E3349–E3358 CrossRef Medline
37. Richter, B., Sliter, D. A., Herhaus, L., Stolz, A., Wang, C., Beli, P., Zaffagnini, G., Wild, P., Martens, S., Wagner, S. A., Youle, R. J., and Dikic, I. (2016) Phosphorylation of OPTN by TBK1 enhances its binding to Ub chains and promotes selective autophagy of damaged mitochondria. *Proc. Natl. Acad. Sci. U.S.A.* **113,** 4039–4044 CrossRef Medline
38. Heo, J. M., Ordureau, A., Paulo, J. A., Rinehart, J., and Harper, J. W. (2015) The PINK1-PARKIN mitochondrial ubiquitylation pathway drives a program of OPTN/NDP52 recruitment and TBK1 activation to promote mitophagy. *Mol. Cell* **60,** 7–20 CrossRef Medline

39. Lazarou, M., Sliter, D. A., Kane, L. A., Sarraf, S. A., Wang, C., Burman, J. L., Sideris, D. P., Fogel, A. I., and Youle, R. J. (2015) The ubiquitin kinase PINK1 recruits autophagy receptors to induce mitophagy. *Nature* **524,** 309–314 CrossRef Medline
40. Tumbarello, D. A., Waxse, B. J., Arden, S. D., Bright, N. A., Kendrick-Jones, J., and Buss, F. (2012) Autophagy receptors link myosin VI to autophagosomes to mediate Tom1-dependent autophagosome maturation and fusion with the lysosome. *Nat. Cell Biol.* **14,** 1024–1035 CrossRef Medline
41. Maruyama, H., Morino, H., Ito, H., Izumi, Y., Kato, H., Watanabe, Y., Kinoshita, Y., Kamada, M., Nodera, H., Suzuki, H., Komure, O., Matsuura, S., Kobatake, K., Morimoto, N., Abe, K., *et al.* (2010) Mutations of optineurin in amyotrophic lateral sclerosis. *Nature* **465,** 223–226 CrossRef Medline
42. Rezaie, T., Child, A., Hitchings, R., Brice, G., Miller, L., Coca-Prados, M., Héon, E., Krupin, T., Ritch, R., Kreutzer, D., Crick, R. P., and Sarfarazi, M. (2002) Adult-onset primary open-angle glaucoma caused by mutations in optineurin. *Science* **295,** 1077–1079 CrossRef Medline
43. Osawa, T., Mizuno, Y., Fujita, Y., Takatama, M., Nakazato, Y., and Okamoto, K. (2011) Optineurin in neurodegenerative diseases. *Neuropathology* **31,** 569–574 CrossRef Medline
44. Chalasani, M. L., Kumari, A., Radha, V., and Swarup, G. (2014) E50K-OPTN-induced retinal cell death involves the Rab GTPase-activating protein, TBC1D17 mediated block in autophagy. *PLoS One* **9,** e95758 CrossRef Medline
45. Shen, X., Ying, H., Qiu, Y., Park, J. S., Shyam, R., Chi, Z. L., Iwata, T., and Yue, B. Y. (2011) Processing of optineurin in neuronal cells. *J. Biol. Chem.* **286,** 3618–3629 CrossRef Medline
46. Shim, M. S., Takihara, Y., Kim, K. Y., Iwata, T., Yue, B. Y., Inatani, M., Weinreb, R. N., Perkins, G. A., and Ju, W. K. (2016) Mitochondrial pathogenic mechanism and degradation in optineurin E50K mutation-mediated retinal ganglion cell degeneration. *Sci. Rep.* **6,** 33830 CrossRef Medline
47. Sirohi, K., Chalasani, M. L., Sudhakar, C., Kumari, A., Radha, V., and Swarup, G. (2013) M98K-OPTN induces transferrin receptor degradation and RAB12-mediated autophagic death in retinal ganglion cells. *Autophagy* **9,** 510–527 CrossRef Medline
48. Sundaramoorthy, V., Walker, A. K., Tan, V., Fifita, J. A., Mccann, E. P., Williams, K. L., Blair, I. P., Guillemin, G. J., Farg, M. A., and Atkin, J. D. (2015) Defects in optineurin- and myosin VI-mediated cellular trafficking in amyotrophic lateral sclerosis. *Hum. Mol. Genet.* **24,** 3830–3846 CrossRef Medline
49. Mizushima, N., Yoshimori, T., and Levine, B. (2010) Methods in mammalian autophagy research. *Cell* **140,** 313–326 CrossRef Medline
50. Itakura, E., and Mizushima, N. (2010) Characterization of autophagosome formation site by a hierarchical analysis of mammalian Atg proteins. *Autophagy* **6,** 764–776 CrossRef Medline
51. Tooze, S. A., Dooley, H. C., Jefferies, H. B., Joachim, J., Judith, D., Lamb, C. A., Razi, M., and Wirth, M. (2015) Assessing mammalian autophagy. *Methods Mol. Biol.* **1270,** 155–165 CrossRef Medline
52. Moreau, K., Ravikumar, B., Renna, M., Puri, C., and Rubinsztein, D. C. (2011) Autophagosome precursor maturation requires homotypic fusion. *Cell* **146,** 303–317 CrossRef Medline
53. Ito, H., Nakamura, M., Komure, O., Ayaki, T., Wate, R., Maruyama, H., Nakamura, Y., Fujita, K., Kaneko, S., Okamoto, Y., Ihara, M., Konishi, T., Ogasawara, K., Hirano, A., Kusaka, H., Kaji, R., Takahashi, R., and Kawakami, H. (2011) Clinicopathologic study on an ALS family with a heterozygous E478G optineurin mutation. *Acta Neuropathol.* **122,** 223–229 CrossRef Medline
54. Bento, C. F., Renna, M., Ghislat, G., Puri, C., Ashkenazi, A., Vicinanza, M., Menzies, F. M., and Rubinsztein, D. C. (2016) Mammalian autophagy: How does it work? *Annu. Rev. Biochem.* **85,** 685–713 CrossRef Medline
55. Noda, N. N., Fujioka, Y., Hanada, T., Ohsumi, Y., and Inagaki, F. (2013) Structure of the Atg12-Atg5 conjugate reveals a platform for stimulating Atg8-PE conjugation. *EMBO Rep.* **14,** 206–211 CrossRef Medline
56. Otomo, C., Metlagel, Z., Takaesu, G., and Otomo, T. (2013) Structure of the human ATG12~ATG5 conjugate required for LC3 lipidation in autophagy. *Nat. Struct. Mol. Biol.* **20,** 59–66 Medline
57. Matsushita, M., Suzuki, N. N., Obara, K., Fujioka, Y., Ohsumi, Y., and Inagaki, F. (2007) Structure of Atg5.Atg16, a complex essential for autophagy. *J. Biol. Chem.* **282,** 6763–6772 CrossRef Medline
58. Fracchiolla, D., Sawa-Makarska, J., Zens, B., Ruiter, A., Zaffagnini, G., Brezovich, A., Romanov, J., Runggatscher, K., Kraft, C., Zagrovic, B., and Martens, S. (2016) Mechanism of cargo-directed Atg8 conjugation during selective autophagy. *Elife* **5,** e18544
59. George, S. H., Gertsenstein, M., Vintersten, K., Korets-Smith, E., Murphy, J., Stevens, M. E., Haigh, J. J., and Nagy, A. (2007) Developmental and adult phenotyping directly from mutant embryonic stem cells. *Proc. Natl. Acad. Sci. U.S.A.* **104,** 4455–4460 CrossRef Medline
60. Chalasani, M. L., Radha, V., Gupta, V., Agarwal, N., Balasubramanian, D., and Swarup, G. (2007) A glaucoma-associated mutant of optineurin selectively induces death of retinal ganglion cells which is inhibited by antioxidants. *Invest. Ophthalmol. Vis. Sci.* **48,** 1607–1614 CrossRef Medline
61. Sirohi, K., Kumari, A., Radha, V., and Swarup, G. (2015) A glaucoma-associated variant of optineurin, M98K, activates Tbk1 to enhance autophagosome formation and retinal cell death dependent on Ser177 phosphorylation of optineurin. *PLoS One* **10,** e0138289 CrossRef Medline